

Spin-polarized electron energy loss spectroscopy at high momentum resolution

D. Vasilyev* and J. Kirschner

An improved spin-polarized electron energy loss spectroscopy apparatus with high momentum resolution was developed during the last few years. It is equipped with a multichannel energy analyzer and multichannel spin imaging detector. This technique allows to see features on the energy loss spectra, angular dependence of asymmetry and intensity and pronounced sensitivity on the primary energy. In this work, we studied dipolar scattering resonances, spin-dependent electron-hole excitations and their momentum dependence and collective magnetic excitation, i.e. high energy magnons. Copyright © 2016 John Wiley & Sons, Ltd.

Keywords: spin-polarized; SPEELS; magnetism

Introduction

In magnets, Stoner excitations are related to magnons like electron-hole pairs to plasmons in semiconductors. Stoner excitations can be seen in spin-polarized electron energy loss spectroscopy (SPEELS) as demonstrated 30 years ago.^[1,2] Based on general considerations^[3] and theory,^[4,5] one should expect the energy loss spectrum to be richly structured in intensity and asymmetry as function of energy and angle. The spectra should show features on the scale of 1 eV or less, should depend on the primary energy on a similar scale and should respond to angular variations of a few degrees. However, in experiments with metallic ferromagnets, unanimously, these features were not observed.

During the last few years, we have developed an improved SPEELS apparatus including a multichannel energy analyzer and a multichannel spin detector. The gain in intensity was sacrificed for better angular resolution, and, indeed, all the expected features have been found. We know now that the crucial parameter is momentum resolution, rather than just energy resolution. We found that at least a resolution of 0.1 \AA^{-1} is needed.

Experimental aspects

A schematic view of the SPEELS apparatus is shown in Fig. 1. A spin-polarized electron beam, generated via photoemission from a GaAs-based superlattice, hits the target crystal. The photocathode was cleaned from Ga_2O_3 by atomic hydrogen with simultaneous heating up to 520°C ; then, it was heated up to 550°C for desorption of As_2O_3 .^[6] After that, the cathode was activated by Cs and O_2 according to the standard Yo-Yo procedure. The spin-polarized electrons are excited by circular polarized light from the laser with wavelength of 828 nm, which corresponds to the maximum of polarization in the spectrum. The spin orientation of the primary electrons is changed by variation of the light helicity. Scattered electrons are analyzed with a hemispherical energy analyzer and then hit the delay-line detector.^[7]

The polarization of the electrons can be measured by using a multichannel spin imaging detector. The working principle of the

detector is based on spin-dependent low-energy electron diffraction from single crystalline surfaces. The pseudomorphic Au on Ir (100) is being used as diffraction crystal. This system provides high polarization sensitivity, up to 80%, and more than 7 months of lifetime in ultrahigh vacuum.^[8] Additionally, the magnetization of the target can be changed.

Experimental results

The Ir(100) crystal was used as a target. It was prepared using procedures described in.^[9] For treatment in oxygen, the crystal was heated up to 1200 K under O_2 partial pressure of 8×10^{-8} mbar. Additionally, a short high-temperature flash (about 1600 K) was applied for desorption of oxides. After this procedure, the well-known 5×1 reconstructed surface is visible. Subsequently, the Fe film was evaporated with further annealing at the temperature of 460°C .

The asymmetry obtained for a given direction of sample magnetization contains contributions from spin-orbit (A_{so}) and exchange processes (A_{ex}). By measurement of two asymmetries for opposite directions of the magnetization, one can distinguish between these asymmetries using the equations in the succeeding texts.^[10]

$$A_{\text{ex}} = \frac{A^+ - A^-}{2}; A_{\text{so}} = \frac{A^+ + A^-}{2}$$

A^+ and A^- are the asymmetries for opposite magnetization directions, defined by the equations.

$$A^+ = \frac{N_{\text{pos}}^+ - N_{\text{neg}}^+}{N_{\text{pos}}^+ + N_{\text{neg}}^+}; A^- = \frac{N_{\text{pos}}^- - N_{\text{neg}}^-}{N_{\text{pos}}^- + N_{\text{neg}}^-}$$

where N_{pos} and N_{neg} are the intensities measured for positive and negative helicity of the light respectively.

* Correspondence to: D. Vasilyev, Max-Planck Institut für Mikrostrukturphysik, Weinberg 2, 06120 Halle, Germany.
E-mail: vasilyev@mpi-halle.mpg.de

Max-Planck Institut für Mikrostrukturphysik, Weinberg 2, 06120, Halle, Germany

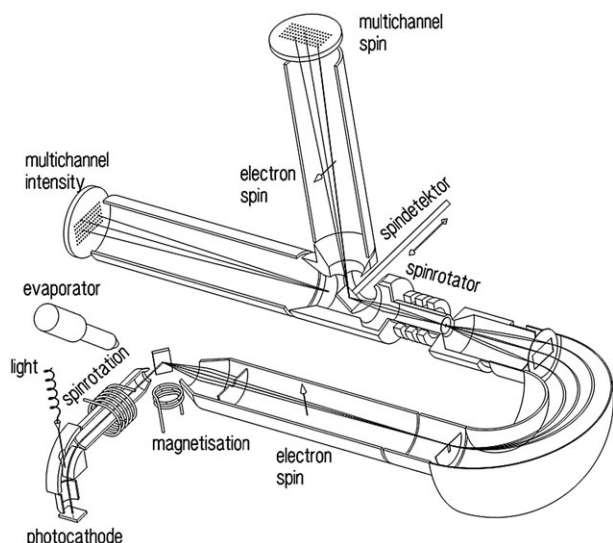


Figure 1. Schematic view of experimental setup for spin-polarized electron energy loss spectroscopy.

Measurements were performed for six monolayers (ML) Fe on Ir (100). In Fig. 2 are shown measured intensity and exchange asymmetry as a function of electron energy loss for target angles (angle with respect to the incidence beam, for the perpendicular incidence, the target angle is 45°) in the range of 4° . One can see that the spectra have different features, for instance an intensity resonance at energy loss of about 2 eV, and we observe a high negative exchange asymmetry at the same energy loss value. With changing of the target angle, the position and shape of curves are changing drastically, the intensity peak decreasing and shifting as well as the asymmetry peak.

In Fig. 3, we present 2D plots for intensity, exchange and spin-orbit asymmetries for two different initial energies. As x and y scale, energy loss and angle with respect to the incident beam respectively were chosen. The resonance is clearly visible on the intensity plot. The exchange asymmetry in the interval from 34° up to around 47° is mostly negative; however, for the higher angles, the positive asymmetry that characterizes Stoner excitations is showing up. It can be seen that by changing the initial energy only by 1 eV, the intensity and exchange asymmetry plots are strongly changing. The resonance shifts toward the lower target angles and higher energy losses. Changes for the exchange asymmetry are mostly visible for angles below 50° , where one also can see a shifting spot of strongly negative asymmetry, which corresponds to the shifting resonance. The spin-orbit asymmetry behavior also changes, but by much less. The results are reproducible not only from one measurement to another but also from one film to another that was prepared using the same procedure. The sensitivity to the remanent magnetization was checked by changing of the discharge voltage of magnetization coil in the range of 7 to 45 V. Once the voltage overcomes the coercivity (the typical value is 15 V), there are no any changes observed for the asymmetry and polarization. From that, we can conclude that the influence of the remanent magnetization is negligible.

In Fig. 4, we show energy loss spectra of exchange asymmetry and intensity measured for initial electron energy of $E_k = 17$ eV and the target angle $\theta = 35^\circ$. Several features are visible on the exchange asymmetry curve. At the energy loss of about 200 meV, we can see a peak of positive asymmetry, which corresponds to the 'magnon tail'. In the presented experiment, it is not possible

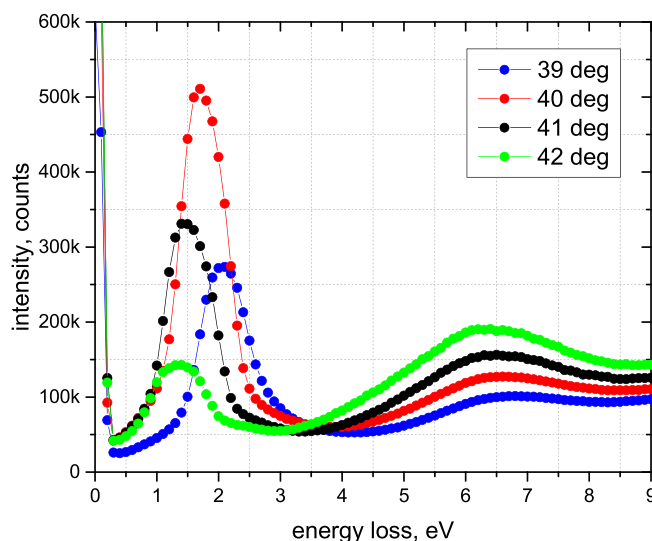
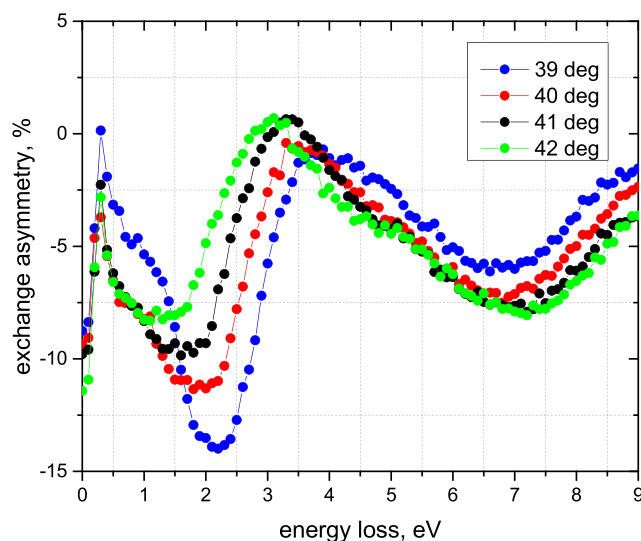


Figure 2. Energy loss spectra of exchange asymmetry and intensity for various angles with respect to the incident beam.

to see the magnon peak fully due to the relatively large width of the elastic peak (about 150 meV); however, the tail is clearly visible. For larger energy loss, one can see a wide region of positive exchange asymmetry that corresponds to the Stoner excitations. These are electron-hole excitations with opposite spin character of electron and hole. In addition at the energy loss of about 5 eV, the resonance and corresponding peak of negative asymmetry is clearly visible.

During the inelastic scattering of spin-polarized electrons, four different processes are possible: two of them are 'spin-flip', denoted by the letter F, and the other two are 'spin-nonflip', denoted by the letter N,

- Fup – electron incident \uparrow ; electron detected \downarrow ,
- Fdown – electron incident \downarrow ; electron detected \uparrow ,
- Nup – electron incident \uparrow ; electron detected \uparrow ,
- Ndown – electron incident \downarrow ; electron detected \downarrow .

To distinguish between these processes, one should know the initial polarization of the beam and measure the polarization of scattered electrons. According to,^[2] normalized transition probabilities can be calculated by the following formulas:

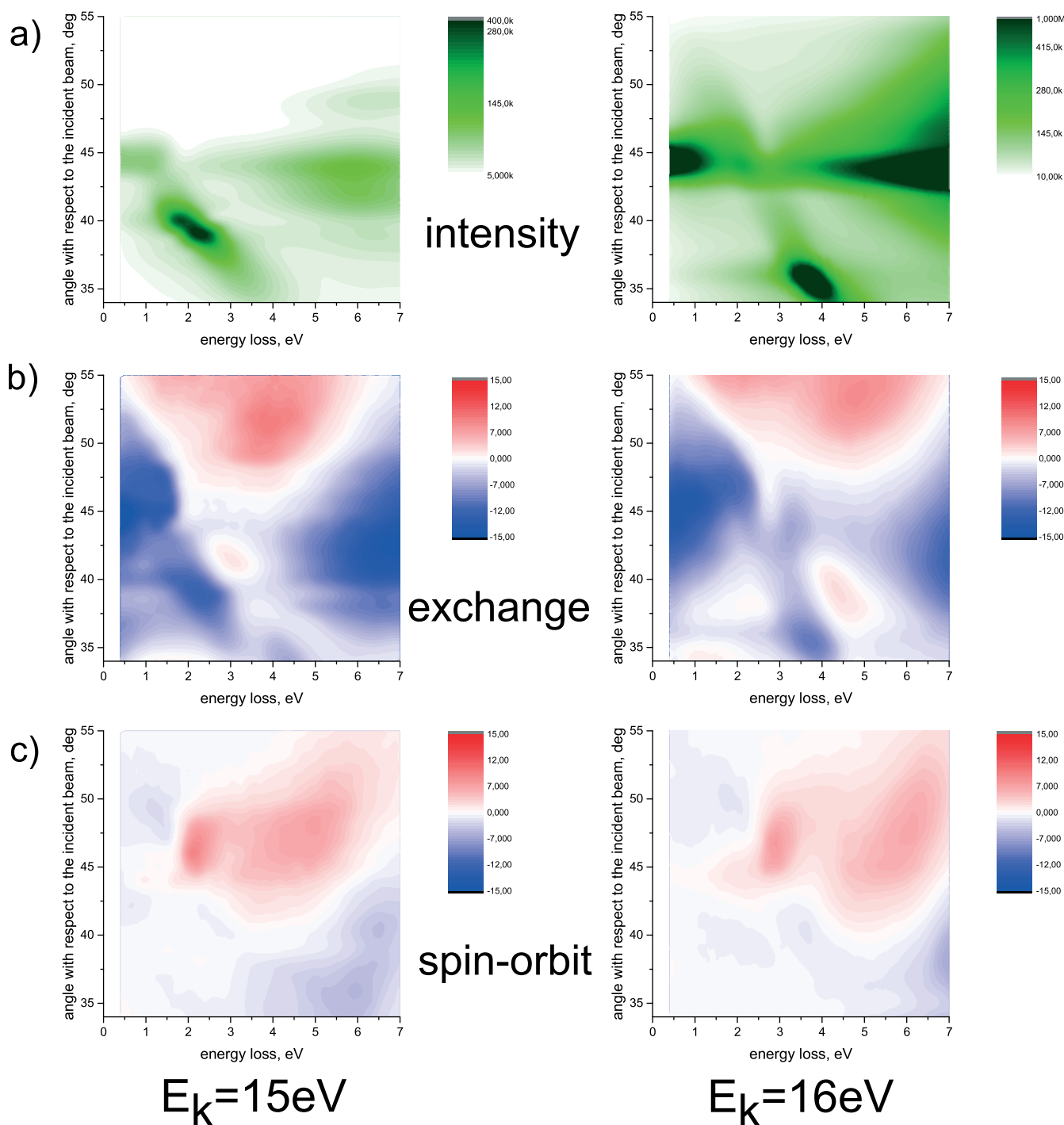


Figure 3. 2D plots of (a) intensity, (b) exchange asymmetry and (c) spin-orbit asymmetry for two different values of the primary electron energy E_k .

$$\begin{aligned}
 F_{\text{up}} &= (1 - \beta_1 - \beta_2 + \beta_3)/4 \\
 F_{\text{down}} &= (1 + \beta_1 - \beta_2 - \beta_3)/4 \\
 N_{\text{up}} &= (1 + \beta_1 + \beta_2 + \beta_3)/4 \\
 N_{\text{down}} &= (1 - \beta_1 + \beta_2 - \beta_3)/4
 \end{aligned}$$

where

$$\beta_1 = \frac{[(1 + A) P_{\text{plus}} + (1 - A) P_{\text{minus}}]}{2 |P_0| D} \quad \beta_2 = \frac{[(1 + A) P_{\text{plus}} - (1 - A) P_{\text{minus}}]}{2 |P_0| D}$$

$$\beta_3 = \frac{A}{|P_0|}$$

where A is the exchange asymmetry, P_{plus} and P_{minus} are final state

spin polarization for initial polarization directed parallel or antiparallel to the orientation of the majority spin in the sample respectively, P_0 is the initial degree of polarization (in our case $P_0 = 0.8$) and D is the detector sensitivity (for our detector, $D = 0.7$).

In Fig. 5, the measured polarization and normalized transition probabilities are shown. The probabilities are normalized such that the sum of all four contributions for each energy loss value give 1. It may be noted that the maximum of polarization corresponds to the 0 eV energy loss, i.e. the elastic peak. That is due to the dominating Coulomb interaction, which does not depend on electron spin. We also can see that in the transition probabilities, at the elastic peak,

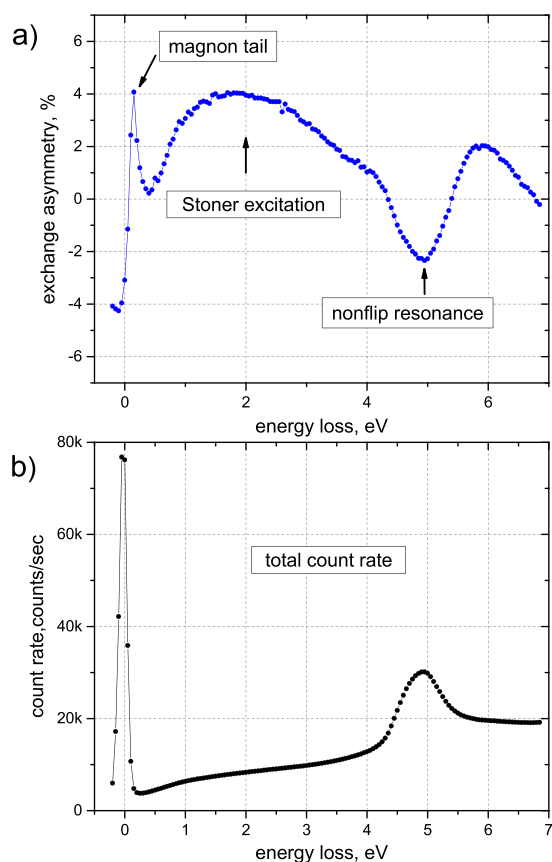


Figure 4. Experimental results for six monolayer Fe on Ir(100), $E_k = 17$ eV, $\theta = 35^\circ$, (a) exchange asymmetry and (b) intensity.

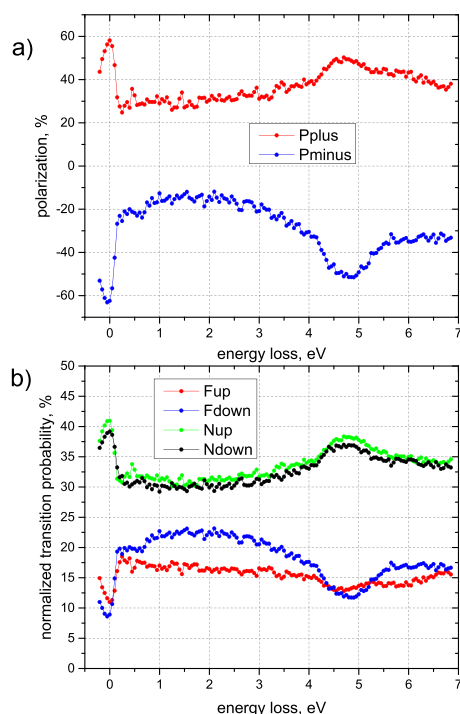


Figure 5. Experimental results for six monolayers Fe on Ir(100), $E_k = 17$ eV, $\theta = 35^\circ$, (a) final state polarization P_{plus} and P_{minus} for initial polarization directed parallel or antiparallel to orientation of the majority spin in the sample respectively and (b) normalized transition probabilities.

the spin-nonflip processes have a maximum, while spin-flip processes have a minimum. Another maximum of polarizations can be seen at the position of the resonance. At this point, the spin-nonflip probabilities have maximum, and spin-flip have minimum as well as for the elastic peak. From this, we can conclude that the spin-nonflip processes are responsible for this resonance. For the Stoner region, dominating of F_{down} over F_{up} is observed.

Conclusion

In conclusion, we can say that spin-polarized energy loss spectroscopy allows to see features on the scale of 1 eV, angular dependence of asymmetry and intensity and pronounced sensitivity on the primary energy. In the past, there has been much speculation why all these features were absent in actual experiments. Our result proves that it needs adequate momentum resolution to discern the momentum-dependent structures in electron energy loss spectroscopy. Our apparatus has an overall momentum resolution of 0.04 \AA^{-1} as determined experimentally. This should not be considered the ultimate value because recent momentum-resolved photoemission demonstrates angle-dependent emission structures on a scale well below 0.001 \AA^{-1} .^[11] The present status calls for a quantitative theory of spin-polarized two-electron transitions within the near-surface band structure of itinerant ferromagnets.

References

- [1] J. Kirschner, *Phys. Rev. Lett.*, **1985**, *55*, 973.
- [2] D. Venus, J. Kirschner, *Phys. Rev. B*, **1988**, *37*, 2199.
- [3] K. P. Kämper, D. L. Abraham, H. Hopster, *Phys. Rev. B*, **1992**, *45*, 14355.
- [4] D. L. Mills, *Phys. Rev. B*, **1986**, *34*, 6099.
- [5] R. Saniz, S. P. Apell, *J. Electr. Spectr. Rel. Phen.*, **2002**, *122*, 139.
- [6] V. Tioukine, K. Aulenbacher, E. Riehn, *AIP Conf. Proc.*, **2009**, *1149*, 1002.
- [7] This prototype apparatus was developed in collaboration with SPECS, Berlin, Germany www.specs.de. **2014**.
- [8] D. Vasilyev, C. Tusche, F. Giebels, H. Gollisch, R. Feder, J. Kirschner, *J. Electr. Spectr. Rel. Phen.*, **2015**, *199*, 10–18.
- [9] R. G. Musket, W. McLean, C. A. Colmenares, D. M. Makowiecki, W. J. Siekhaus, *Appl. Surf. Sci.*, **1982**, *10*, 143.
- [10] S. F. Alvarado, R. Feder, H. Hopster, F. Cicacci, H. Pleyer, *Z. Phys. B – Condensed Matter*, **1982**, *49*, 129–132.
- [11] C. Tusche, A. Krasnyuk, J. Kirschner, *Ultramicroscopy* (**2015**) 10.1016/j.ultramicro.2015.03.020k